Analytica Chimica Acta 1107 (2020) 40–47

Contents lists available at ScienceDirect

Analytica Chimica Acta

journal homepage: www.elsevier.com/locate/aca

A novel nest hybridization chain reaction based electrochemical assay for sensitive detection of circulating tumor DNA

YiFang Huang [a, b, 1], MaLiang Tao [a, b, 1], ShiHua Luo [a, b], Ye Zhang [a, b], Bo Situ [a, b], XinYi Ye [a, b], PeiWen Chen [a, b], XiuJuan Jiang [a, b], Qian Wang [a, b, **], Lei Zheng [a, b, *]

[a] Department of Laboratory Medicine, Nanfang Hospital, Southern Medical University, Guangzhou, 510515, Guangdong Province, PR China
[b] Guangdong Engineering and Technology Research Center for Rapid Diagnostic Biosensors, Nanfang Hospital, Southern Medical University, Guangzhou, 510515, Guangdong Province, PR China

HIGHLIGHTS

- A novel electrochemical assay for detection of circulating tumor DNA is proposed.
- The assay takes advantages of nest hybridization chain reaction for signal amplification.
- The biosensor exhibits high sensitivity and specificity for ctDNA detection.
- This biosensor has been applied in the detection of ctDNA in clinical samples and holds great potential in cancer diagnosis.

GRAPHICAL ABSTRACT

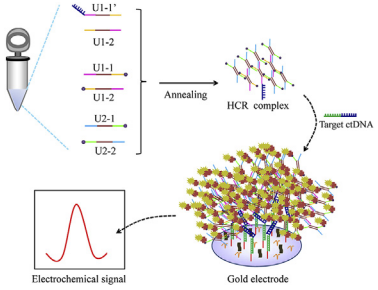

ARTICLE INFO

Article history:
Received 3 December 2019
Received in revised form
13 January 2020
Accepted 3 February 2020
Available online 5 February 2020

Keywords:
Circulating tumor DNA
Electrochemical biosensor
Nest hybridization chain reaction
Cancer diagnosis

ABSTRACT

As an ideal biomarker candidate, circulating tumor DNA (ctDNA) plays a vital role in noninvasive diagnosis of cancer. However, most traditional approaches for quantifying ctDNA are cumbersome and expensive. In the present work, a novel electrochemical biosensor based on nest hybridization chain reaction was proposed for the sensitive and specific detection of PIK3CA E545K ctDNA with a simple process. The nest hybridization chain reaction was initiated by the hybridization of two dumbbell-shaped DNA units which were assembled by two classes of well-designed DNA probes respectively, leading to the formation of a complex DNA structure. In the presence of target ctDNA, the amplified hybridization chain reaction products were captured by target ctDNA, resulting in a significant increase of electrochemical signal. Under the optimal conditions, the developed biosensor exhibited good analytical performance for the detection of target ctDNA with the linear range from 5 pM to 0.5 nM and the detection limit of 3 pM. Furthermore, this assay was successfully applied to the detection of ctDNA in spiked-in samples, pleural effusion and serum samples of malignant tumor patients. This simple and cost-effective sensing system holds great potentials for ctDNA detection and cancer diagnosis.

* Corresponding author. Department of Laboratory Medicine, Nanfang Hospital, Southern Medical University, Guangzhou, 510515, Guangdong Province, PR China.
** Co-corresponding author. Department of Laboratory Medicine, Nanfang Hospital, Southern Medical University, Guangzhou, 510515, Guangdong Province, PR China.
E-mail addresses: nfyywangqian@163.com (Q. Wang), nfyyzhenglei@smu.edu.cn (L. Zheng).
[1] These authors contributed equally to this work.

https://doi.org/10.1016/j.aca.2020.02.006
0003-2670/

1. Introduction

Circulating tumor DNA (ctDNA) is small DNA fragments in peripheral blood circulation that is released from solid tumor cells [1,2]. CtDNA has attracted a lot of attention because it carries tumor-associated alterations, such as point mutations and copy number variations (CNV) [3,4]. Importantly, with a short half-life from 2 h to one day in peripheral blood, ctDNA holds great promise to be used for real-time monitoring of the chronic changes and therapeutic response of tumors [2,5]. Furthermore, ctDNA samples can be easily, repeatedly obtained from circulation of patients with a nearly noninvasive sampling process [6]. Given that, ctDNA analysis brings a new insight into liquid biopsy detection of cancer. However, the detection and characterization of ctDNA in serum of cancer patients is often challenging and time-consuming, owing to the low fraction of ctDNA (~1.0%) and the high levels of wide-type DNAs [7].

Conventional methods for ctDNA detection are mainly divided into two categories: Polymerase chain reaction (PCR)-based methods and sequencing-based methods [2,5,8,9]. PCR-based methods, including real-time PCR and digital PCR, have been suggested as effective methods for quantifying ctDNA [10,11]. However, these methods are not well suitable for detecting short fragment ctDNA (less than 100 base pairs) because such methods usually require a high integrity of the template DNA. In addition, the whole process of PCR assays, especially ddPCR, is complex and tedious, which may restrict their further applications. Whole genome sequencing is comprehensive enough for mutation analysis of ctDNA and has been applied in a large scale of studies [5,8]. Unfortunately, it is costly and also requires cumbersome processes. Therefore, an easy-to-operate assay with high sensitivity and specificity is needed for the assessment of ctDNA.

To circumvent these problems, many enzyme-free, isothermal amplification methods have been developed, such as hybridization chain reaction (HCR), catalytic hairpin assembly (CHA), rolling-circle amplification (RCA) and strand-displacement amplification (SDA) [12–16]. Among them, HCR is attractive because of its several advantages, such as low cost, easy operation and superior signal amplification performance [17–19]. Based on these unique properties, improved HCR strategies have been proposed for the detection of multiple molecular targets, including cell free DNA, tumor cells, miRNA and proteins [20–25]. Nevertheless, in those traditional HCR-based electrochemical systems, the charge transfer process is largely limited by the long distance between the enzyme on linear DNA polymer and the electrode surface [26]. Additionally, the leakage of hairpins in traditional HCR is still not well addressed [27].

In an effort to address these problems, we proposed a novel HCR system based on nonlinear amplification by introducing three different classes of dumbbell-shaped DNA probes. The inter-reaction of DNA probes could result in the formation of a complex nest DNA structure [28]. The formation of this nest DNA nanostructure is helpful for reducing the distance between the gold electrode surface and the reaction substrate in electrochemical system, thereby promoting charge transfer process. PIK3CA E545K ctDNA, a remarkable biomarker in breast cancer, was used as a model [29]. Without target ctDNA, the complex DNA structure could not attach to the Au-electrode surface and no electrochemical signal could be detected. In the presence of target ctDNA, HCR polymer could be captured and an obvious current signal could be achieved with the help of biotin-avidin system. This new method combines the nest HCR with electrochemical platform for the first time. The assay we presented here may emerge as a promising and convenient platform for ctDNA detection with high sensitivity and specificity.

2. Experiment section

2.1. Reagents

All oligonucleotides used in our study were synthesized and purified by Sangon Biotechnology Co. Ltd. (Shanghai, China), and the sequences are listed in Table 1. 6-mer-capto-1-hexanol (MCH), bovine serum albumin (BSA), and streptavidin-alkaline phosphatase (ST-AP) were purchased from Sigma-Aldrich (St. Louis, MO, USA). 20 bp DNA Marker was purchased from TakaRa Biotech (Dalian, China). The saline-sodium citrate (SSC) buffer was purchased from Sangon Biotechnology Co. Ltd. (Shanghai, China) and polyacrylamide/bis (30% w/v) were from Thermo Fisher Scientific (MA, USA). All reagents were of analytical reagent grade and all aqueous solutions used in the whole experimental process were prepared with Milli-Q water (≥18 MΩ, Milli-Q, Millipore). Tris-HCl buffer (20 mM Tris, 0.1 M NaCl, 5.0 mM $MgCl_2$ and 0.05% Tween-20, pH 7.40) and Diethanolamine (DEA) buffer (0.1 M DEA, 1 M $MgCl_2$ and 0.1 M KCl, pH 9.6) were used as washing buffer. 2 × SSC buffer was employed as hybridization buffer.

2.2. Apparatus

Electrochemical measurements were measured on a CHI660E electrochemical workstation (Shanghai Chenhua Instruments Co. Ltd., China) with a conventional three-electrode system. Electrochemical impedance spectroscopy (EIS) and square wave voltammetry (SWV) were performed in 3 mL 5.0 mM $[Fe(CN)_6]^{3-/4-}$ solution. Differential pulse voltammetry (DPV) measurements were carried out in 3 mL of DEA solution containing 1 mg mL^{-1} of α-NP. PAGE electrophoresis was performed on an electrophoresis analyzer (Bio-Rad, USA) and the gel was imaged on Gel Doc XR + system (Bio-Rad, USA).

2.3. Preparation of probes

The HCR probes were designed based on the principle of hybridization chain reaction and their structures were tested using the NUPACK design tools (http://www.nupack.org/) [28]. All oligonucleotides were dissolved in TE buffer (10 mM Tris, 1 mM ethylenediaminetetraacetic acid (EDTA), pH = 8.0). The nest HCR system consisted of four basic DNA probes (U1-1, U1-2, U2-1 and U2-2), capture probes on the surface of electrodes, and SSC buffer. First, 10 μM U1-1 and 10 μM U1-2 were mixed in 2 × SSC buffer to construct DNA unit, U1. The hybridization process was performed in Mastercycler® X50s thermocycler (Eppendorf, Hamburg, Germany) as follows: denatured at 95 °C for 5 min, then annealed at 50 °C for 10 min and further annealed at 37 °C for 10 min. Similarly, U2 was constructed by mixing U2-1 and U2-2 in 1:1 in 2 × SSC buffer. Then, 2 μl U1 and 2 μl U2 were mixed in 16 μl 2 × SSC hybridization buffer. The mixture was reacted at 42 °C for 30 min and the annealed U1–U2 products were stored at room temperature until used.

2.4. Preparation of electrochemical biosensor

The 2 mm bare gold electrodes (Shanghai Chenhua Instruments Co. Ltd., China) was polished with 0.05 μm alumina slurries and ultrasonically cleaned in ultrapure water for 15 min, then treated with piranha solution (H_2O_2:H_2SO_4 = 1:3 v/v) for 10 min to remove surface contaminants. Afterward, the pretreated gold electrode was rinsed with Tris-HCl buffer for 3 times and dried at room temperature. 10 μL of thiolated capture probes (0.2 μM) were placed onto cleaned gold electrode surface for 15 h at 4 °C. The gold electrode was then rinsed with Tris-HCl washing buffer for 3 times. After modification, the electrode was treated with 10 μL MCH (1 mM) for

Table 1
DNA sequences of used in this assay.

Name	Sequence
Capture Probe	5′−SH−$(CH_2)_6$ TTTTTTTTTTAGATCCTCTCTCTA-3′
U1-1′	5′-AAATCACTGAGCAGGACTAGCTCATACATCATCCTATCTATCCAGACTCTCACACGTACTC -3′
U1-1	5′-CTAGCTCATACATCATCCTATCTATCCAGACTCTCACACGTACTC-biotin -3′
U1-2	5′-CTAGCTCATACATCGTCTGGATAGATAGGATTCTCACACGTACTC-3′
U2-1	5′-GATGTATGAGCTAGGAGATGCAATCGACTGTGAGTACGTGTGAGA-biotin -3′
U2-2	5′-GATGTATGAGCTAGACAGTCGATTGCATCTC GAGTACGTGTGAGA-3′
PIK3CA E542K ctDNA	5′-CTCAGTGATTTTAGAGAGAGGAT-3′
ctDNA(1)	5′-CTCAGTGATTTAAGAGAGAGGAT-3′
ctDNA(2)	5′-CTCAGAGATTTAAGAGAGAGGAT-3′
ctDNA(3)	5′-CTCAGTGATTTAAGAGTGAGGAT-3′
ctDNA(4)	5′-CTCAGAGATTTAAGAGTGAGGAT-3′

1 h to obtain well-aligned DNA monolayer. After rinsing with washing buffer, the electrode was treated with 2% BSA for 30 min to block the uncovered region and prevent nonspecific binding of oligonucleotides. After that, the modified electrode was incubated with 10 μL of different concentrations of ctDNA for 30 min. The Au/capture DNA/MCH/BSA/ctDNA electrode was obtained [30].

Subsequently, the Au/capture DNA/MCH/BSA/ctDNA electrode was incubated with prepared HCR products for 30 min and washed with DEA buffer containing 0.05% Tween-20 for 3 times. After that, 10 μL of 0.9 g mL^{-1} of ST-AP was added to the electrode surface at 37 °C for 30 min. After washing with DEA buffer containing 0.05% Tween-20, the resulted Au/capture DNA/MCH/BSA/ctDNA/HCR/ST-AP was used for the sensing interface. The differential pulse voltammetry (DPV) measurements were carried out in DEA buffer containing 1 mg mL^{-1} of α-NP. The modulation time of DPV measurements was 0.05 s, interval time was 0.017 s, and step potential scan was from 0 to +0.6 V (Scheme 1).

2.5. PAGE electrophoresis

10 μL of HCR products were mixed with 2 μL of 6 × loading buffer and analyzed by 12% native polyacrylamide gel electrophoresis (PAGE) in 0.5 × TBE buffer (45 mM tris-boric acid, 1 mM EDTA, pH 8.3). Gel electrophoresis was run at 130 V constant voltage for 40 min and stained with 1 × 4S red plus nucleic acid stain for 40 min. Finally, the gels were analyzed using Gel Doc XR + system (Bio-Rad, USA).

2.6. Clinical samples preparation

Blood samples were collected from 23 breast cancer patients and 24 healthy controls (Nanfang Hospital, Southern Medical University). Serum was separated by centrifugation at 2200 g for 10 min at 4 °C. Pleural effusion samples were harvested from 25 hepatocellular carcinoma patients. Cell free DNA in serum and pleural effusion was isolated using the QIAamp Circulating Nucleic Acid kit (QIAGEN, Germantown, MD) following the manufacturer's instructions. The quality of cell free DNA was assessed using a NanoDrop 2000c spectrophotometer (Thermo Fisher Scientific, Inc., Waltham, MA, USA). A total of 100 ng cell free DNA of each sample was incubated with capture probe on gold electrode surface. The Au/capture DNA/ctDNA electrode was incubated with HCR products and used for DPV analysis, as described above.

3. Results and discussion

3.1. Principle of the nest HCR-based electrochemical sensor

The novel HCR sensing system is composed of three dumbbell-shaped DNA unites (U1′, U1 and U2), capture probes and gold electrodes. The principle of our HCR strategy is illustrated in Scheme 1. The dumbbell-shaped DNA unites (U1′, U1 and U2) are formed by three different pairs of starting oligonucleotides, respectively (U1-1'/U1-2, U1-1/U1-2 and U2-1/U2-2). DNA units U1 and U2 are designed to have two sets of sticky ends that are complementary to each other. To detect the target ctDNA, DNA unit U1' is designed on the basic of U1 to have one sticky end complementary to the target ctDNA. With complementary sticky ends, these DNA unites can bind to each other, resulting in the formation of a complex nest DNA structure after n cycles of reaction. In the presence of target ctDNA, capture probes can bind to ctDNA specifically, and the nest HCR products are then hybridized with a second part of ctDNA. Finally, these biotinylated HCR products can react with ST-AP and AP catalyzes the substrate α-NP to electroactive products. As a result, the electrochemical signal is significantly amplified and can be quantified by differential pulse voltammetry (DPV) in electrochemical system. In contrast, the HCR products cannot be captured without ctDNA, resulting in a low electrochemical signal.

3.2. Probe design principle and feasibility of the HCR strategy

The detail structure of starting probes and the reaction principle of HCR are depicted in Fig. 1A. Each probe is composed of three parts: middle segment, 5′ ends and 3' ends. The middle sequences, 1 and 1c (or 4 and 4c), are complementary to each other, and the sticky ends of U1-1/U2-1 have the same sequence as those in U1-2/U2-2. The DNA unites (U1 and U2) are designed to have complementary ends to hybridize with each other (2 and 2c, 3 and 3c). Theoretically, one unit of U1 hybridizes with four units of U2, and the continued hybridization of U1 and U2 lead to the successful HCR process. Thus, a large nest DNA structure is assembled by mixing these two DNA unites (U1 and U2) together. According to the above principle, U1 (U1-1 and U1-2) and U2 (U2-1 and U2-2) were designed and their structures are shown in Fig. S1.

To evaluate the feasibility of the proposed electrochemical HCR system, DPV measurements were investigated with different ratios of input U1 and U2 units. As shown in Fig. 1C and D, DPV peak current showed a very weak current signal when U1 and U2 were absence (curve d). When U1 was modified on the surface of electrode, the current increased a little (curve c). When U1 and U2 units were both present, a significantly increased current was observed (curve a and b). It was due to the fact that HCR was triggered by the hybridization of U1 and U2 and the products were introduced onto the electrode surface, resulting in the enhanced signal output. It was noted that the current response of HCR products formed by mixing U1 and U2 in a ratio of 1:1 (curve a) was much higher than that of 1:4 (curve b). This was because HCR products were fully formed in the presence of sufficient U1 and U2, while the yield of large HCR products was reduced with insufficient U1. The results

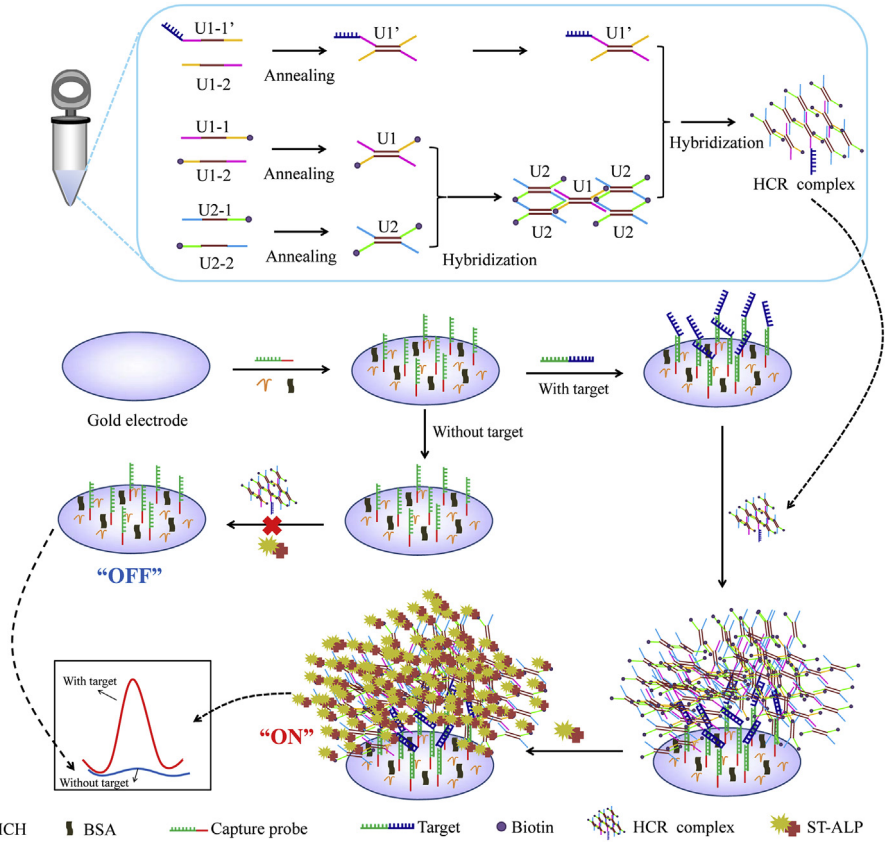

Scheme 1. Schematic illustration of the electrochemical sensor for detecting ctDNA based on nest hybridization chain reaction. Firstly, dumbbells shaped DNA unites (U1′, U1 and U2) were constructed by annealing of specific oligonucleotides, respectively. Then, the DNA unites were mixed together in a certain proportion to form complex nest-like HCR products. The thiolated capture probes were immobilized onto gold electrode surface. Target ctDNA could be captured by these capture probes. The sticky end of U1′ in the nest-like HCR products was also complementary to a second part of ctDNA, enabling HCR products to bind to the gold electrode surface. The biotinylated HCR products can react with ST-AP and AP catalyzes the substrate α-NP to electroactive products. As a result, an obvious current signal could be detected in the presence of target ctDNA and a low signal in the absence of ctDNA.

indicated that the novel nest HCR system could amplify the signal significantly and is feasible for downstream applications.

The products and the sequences of the HCR system were also investigated by PAGE. As shown in Fig. 1B, lane 1 to lane 4 with two classes of starting probes showed one band. As expected, two DNA unites (U1 and U2) were formed by mixing the starting probes at a ratio of 1:1 (lane 5 and lane 6). When U1 and U2 were mixed, a band above U1 and U2 was generated (lane 7 to lane 9), indicating the formation of U1–U2 complexes. Particularly, a ratio of 1:1 (land 7) for U1 and U2 showed a brighter band than that of 1:4 (land 8) and 1:10 (land 9). The excessive amount of U2 resulted in a 80 bp band in lane 8 and lane 9, while this band was not detectable in land 7. These results were in good agreement with the DPV results. All these findings demonstrated the successful and accurate assembly of the established nest HCR system.

3.3. Characterization of the modified electrode

In order to investigate the DNA assembly on gold electrode, electrochemical impedance spectroscopy (EIS) and square wave voltammetry (SWV) were measured. The EIS measurements were performed in the 0.5 mM $K_3[Fe(CN)_6]$ solution containing 0.4 M KCl and the electron-transfer resistance (Ret) was calculated by the Nyquist plots [25,30]. As depicted in Fig. 2A, points represented individual EIS measurements and the curves showed the simulated results. A low Ret signal was observed for bare Au electrode (Fig. 2A, curve a), indicating a fast electron transfer process. A good electrochemical conductivity of the bare electrode was observed in SWV (Fig. 2B, curve a). After the electrode was modified by capture probe, the Ret increased slightly (Fig. 2A, curve b). This was because the negatively charged DNA probes on the electrode surface led to electrostatic repulsion of $K_3[Fe(CN)_6]$ [31,32]. Compared with bare electrode, the conductivity of the capture DNA modified electrode was reduced in SWV (Fig. 2B, curve b). After modification of MCH and BSA, the Ret continually increased (Fig. 2A, curve c) and the conductivity kept decreased (Fig. 2B, curve c) because the biological molecules hindered the electron-transfer. The Ret continued to increase with the immobilization of the target ctDNA (Fig. 2A, curve d). As the target ctDNA combined with the capture probe, the electron-transfer efficiency decreased with the introducing of negatively charged DNA (Fig. 2B, curve d). Especially, a remarkable increase in the Ret signal was observed after incubating with U1–U2 complexes (Fig. 2A, curve e), owing to the fact that the large DNA structures led the impedance increased significantly. As a result, the conductivity was decreased (Fig. 2B, curve e), suggesting the successful assembly and amplification of our HCR biosensor.

3.4. Optimization of assay conditions

The reaction time and temperature are important factors for the HCR system. To obtain the best sensing performance, these important analytical parameters were optimized with 10 nM target ctDNA. The DPV current signal was detected with different hybridization time of U1 and U2 in the range from 10 min to 50 min

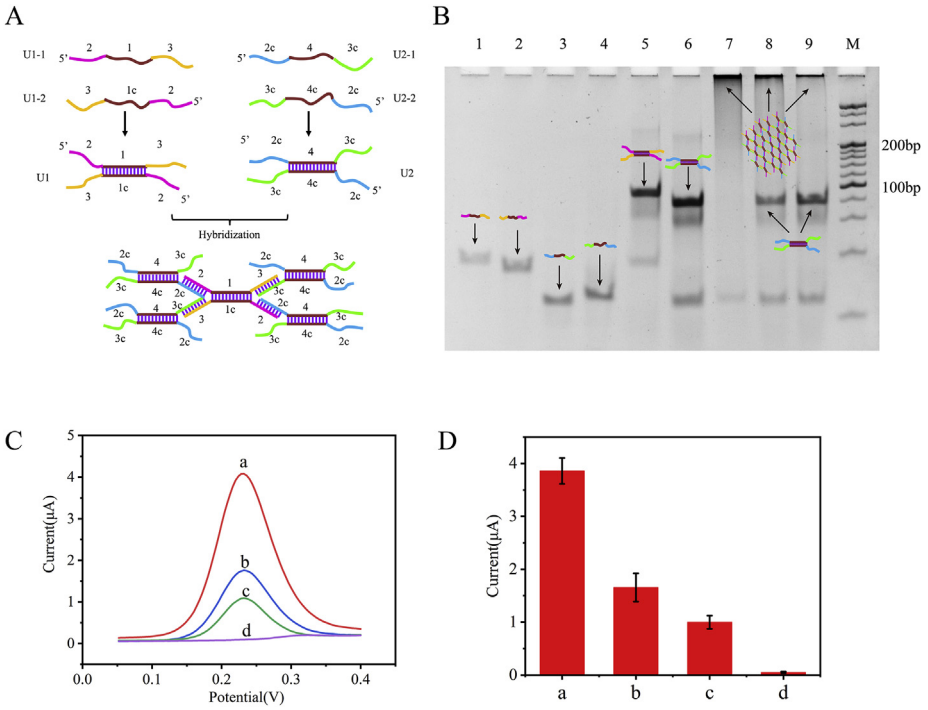

Fig. 1. (A) Schematic illustration of the nest HCR designed principle. The structure of two starting probes and inter-reaction of DNA units were showed. (B) Native PAGE analysis of the HCR products. Lane 1: U1-1 (1 μM); Lane 2: U1-2 (1 μM); Lane 3: U2-1 (1 μM); Lane 4: U2-2 (1 μM); Lane 5: U1 (1 μM); Lane 6: U2 (1 μM); Lane 7: U1: U2 = 1:1 (1 μM U1 and 1 μM U2); Lane 8: U1:U2 = 1:4 (250 nM U1 and 1 μM U2); Lane 9: U1:U2 = 1:10 (100 nM U1 and 1 μM U2); Lane M: 20 bp marker. The reaction temperature for HCR was 42 °C and the incubation time was 30 min. (C) Typical DPV responses and (D) DPV peak currents under different conditions of (a) U1:U2 = 1:1 (50 nM U1 and 50 nM U2), (b) U1:U2 = 1:4 (12.5 nM U1 and 50 nM U2), (c) only U1 (50 nM), and (d) blank control (aqueous solution). The reaction temperature for HCR was 42 °C and the incubation time was 30 min.

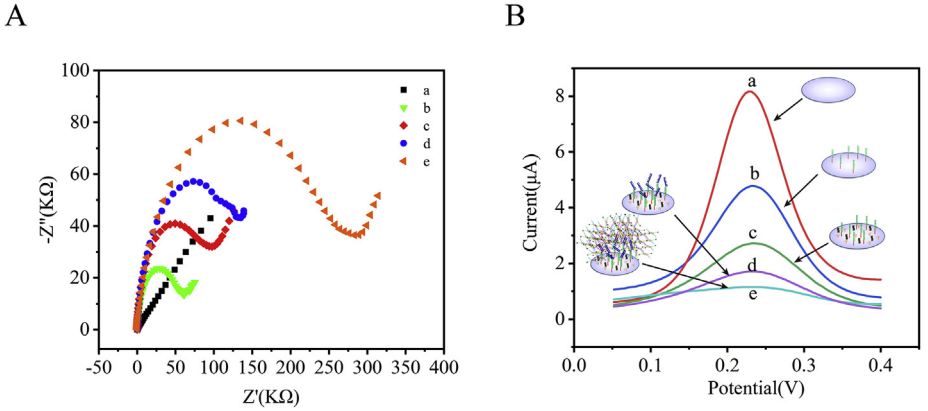

Fig. 2. EIS (A) and SWV (B) responses in 0.5 mM $K_3[Fe(CN)_6]$ solution containing 0.4 M KCl at different modification processes: (a) bare electrode, (b) electrode modified by 10 μL of 0.2 μM capture probes, (c) 10 μL of 1 mM MCH and 2% BSA modified electrode, (d) 10 μL of 50 nM ctDNA hybridized with capture probes, (e) ctDNA hybridized with 10 μL of 50 nM U1–U2 complexes.

with 10 min interval. As presented in Fig. S2, the current signal increased with time and reached the plateau stage at 30 min, indicating that 30 min was the optimal hybridization time. Therefore, 30 min was selected as the optimum reaction time for HCR.

Additionally, the reaction temperature also had significant influence on the HCR process. The current signal of this HCR system was investigated from 4 °C to 56 °C, and the best signal was obtained at 42 °C (Fig. S3). At low temperature, the formation of U1–U2 complexes is significantly reduced because of the insufficient energy. At high temperature, the U1–U2 complexes may become unstable. Thus, the optimal temperature of 42 °C was applied in this experiment.

3.5. Analytical capability of the electrochemical biosensor

To assess the sensitivity of the electrochemical biosensor, PIK3CA E545K ctDNA at different concentrations was investigated under the optimal conditions. As indicated in Fig. 3A, the DPV current signal gradually increased along with the increase of ctDNA concentration and reached a maximum at the concentration of 5 nM. As shown in the inset plot in Fig. 3B, a good linear relationship between DPV current and the concentration of ctDNA was observed in the range of 5 pM–0.5 nM; the linear regression equation was $D = 2.2338 + 0.9125\log_{10}C$ with a linear correlation coefficient of 0.9973, where D was the DPV current and C was the

concentration of ctDNA. The detection limit of ctDNA was estimated to be 3 pM based on the signal of blank tests and the standard deviation. Such low detection limit was in comparable range with previous assays for ctDNA detection [14,29,33]. These results suggested that the highly sensitive electrochemical biosensor for ctDNA detection can be realized.

Furthermore, in order to estimate the specificity of the proposed electrochemical biosensor, four kinds of mismatched DNA (shown in Table 1), namely ctDNA(1), ctDNA(2), ctDNA(3), ctDNA(4), were designed to compare with ctDNA at a concentration of 10 nM. As demonstrated in Fig. 3C and D, the DPV signal was decreased clearly in mismatched DNAs compared with ctDNA, and the shifts in the peak current were 3.22 μA (ctDNA versus ctDNA (1)), 3.80 μA (ctDNA versus ctDNA (2)), 4.31 μA (ctDNA versus ctDNA (3)), 4.47 μA (ctDNA versus ctDNA (4)) and 4.49 μA (ctDNA versus blank), respectively. It was easy to distinguish ctDNA from the one-base mismatched ctDNA(1) and two-base mismatched ctDNA(2), ctDNA(3). In addition, the current signal was very weak in DNA sequences with three or more mismatched bases, which was comparable to that in the blank solution. These results indicated that the current signal was specifically amplified by the target ctDNA, suggesting that the HCR electrochemical biosensor exhibited good performance for discriminating ctDNA from other nucleotides.

3.6. Detection in clinical samples

To further evaluate the clinical application potentiality of our electrochemical biosensor, serum samples from healthy people spiked with different concentrations of PIK3CA E545K ctDNA were analyzed. The DPV current detection was performed under the optimal experimental conditions described above. As the results shown in Fig. 4A and B, an exponential trend curve between DPV current and the concentration of ctDNA in spiked-in samples was observed, which was similar to that in TE buffer. The DPV current enhancement was observed when PIK3CA E545K ctDNA was present and the detectable concentration was as low as 0.5 nM. As shown in the inset plot in Fig. 4B, a linear relationship was observed in the range of 0.5 nM−50 nM; the equation of regression line was D = 0.0579C-0.082, with a linear correlation coefficient of 0.9463, where D was the DPV current and C was the concentration of ctDNA. In addition, as the enrichment of ctDNA also plays an important role in improving the detection limit of the biosensor, a more powerful enrichment method is needed to improve the sensitivity of the biosensor in further studies.

Furthermore, the biosensor was also used to detect ctDNA in 72 clinical samples, including 25 pleural effusion samples from hepatocellular carcinoma patients, 23 serum samples from breast cancer patients and 24 serum samples from healthy individuals. As shown in Fig. 4C, a low current signal (<0.21 μA) was detected in all healthy individuals, whereas the DPV responses increased significantly in 6 samples from breast cancer patients and 2 pleural effusion samples from hepatocellular carcinoma patients. The range of current in these samples was from 0.38 μA to 1.15 μA. The concentration of ctDNA in clinical samples could be calculated by using the regression equation of spiked-in samples (Table S1). The DPV signal enhancement may be attributed to the presence of PIK3CA E545K ctDNA in these malignant samples. This result of high PIK3CA E545K frequency in breast cancer samples is consistent with previous studies [34]. Therefore, the above results demonstrated that this novel HCR electrochemical biosensor exhibits good performance and may be applied to ctDNA analysis in serum samples and pleural effusion samples.

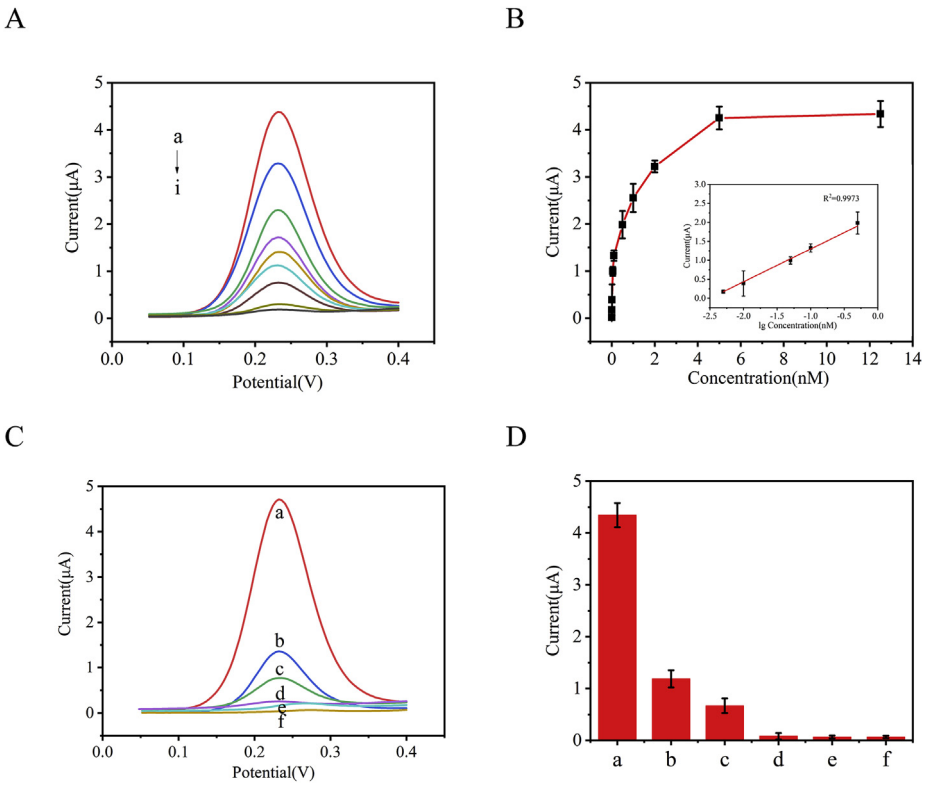

Fig. 3. (A) DPV responses and (B) The calibration curve of the electrochemical biosensor to different concentrations of target ctDNA. From a to i: 5 nM, 2 nM, 1 nM, 0.5 nM, 0.1 nM, 0.05 nM, 0.01 nM, 0.005 nM and 0 nM. (C) Typical DPV responses and (D) DPV peak currents of 10 nM of different target DNA: (a) PIK3CA E542K ctDNA, (b) ctDNA (1) with single-base mismatch, (c) ctDNA (2) with two-bases mismatch, (d) ctDNA (3) with two-bases mismatch, (e) ctDNA (4) with three-bases mismatch, and (f) blank control. The concentration of U1 and U2 for HCR was 50 nM, the reaction temperature was 42 °C and the incubation time was 30 min.

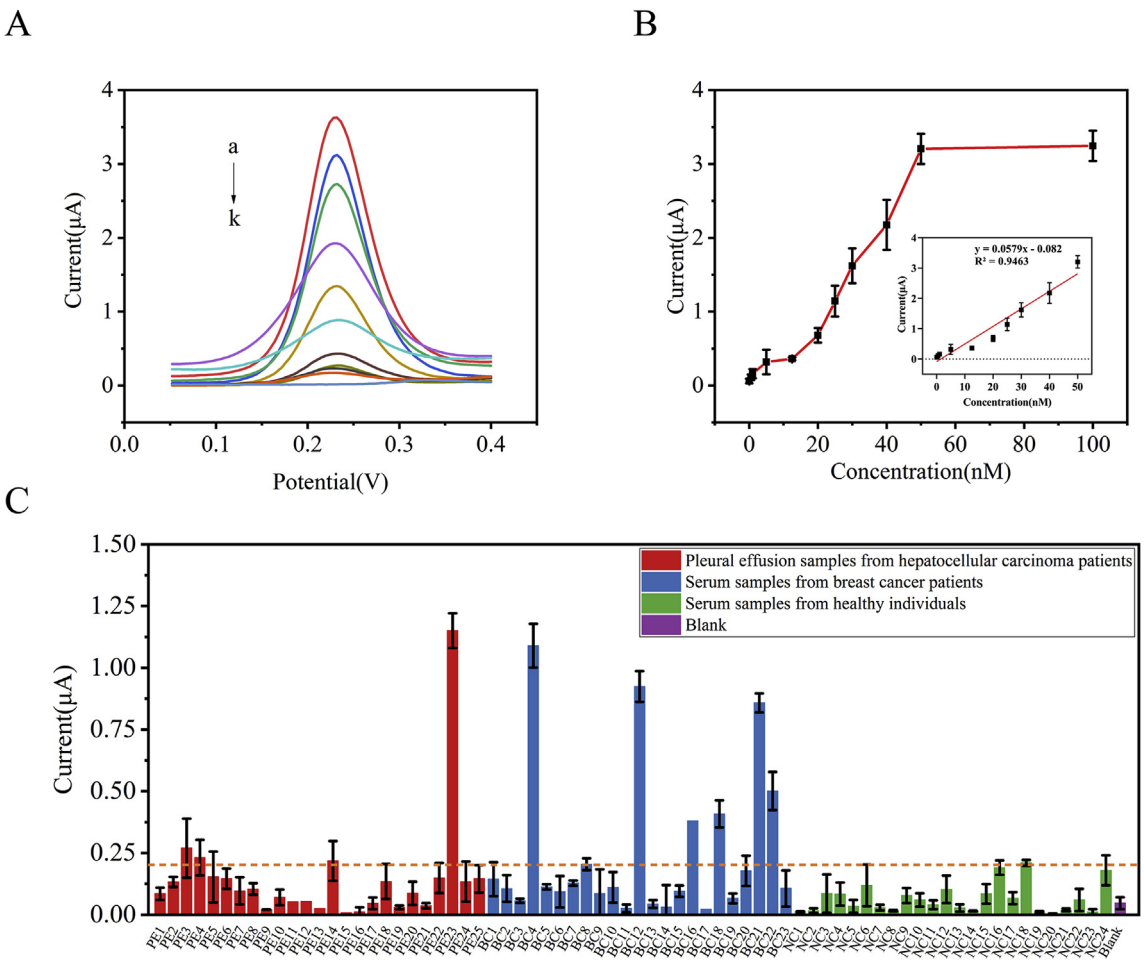

Fig. 4. (A) DPV responses and (B) The calibration curve of different concentrations of target ctDNA spiked in blood samples of healthy donors. From a to k: 100 nM, 50 nM, 40 nM, 30 nM, 25 nM, 20 nM, 12.5 nM, 5 nM, 1 nM, 0.5 nM, and 0 nM. The concentration of U1 and U2 for HCR was 50 nM, the reaction temperature was 42 °C and the incubation time was 30 min. (C) DPV peak currents of the sensor to 100 ng cell free DNA extracted from 25 pleural effusion samples from hepatocellular carcinoma patients, 23 serum samples from breast cancer patients and 24 serum samples from healthy individuals. The concentration of U1 and U2 for HCR was 50 nM, the reaction temperature was 42 °C and the incubation time was 30 min.

4. Conclusion

In conclusion, a rapid and simple electrochemical biosensor based on nest HCR signal amplification strategy has been developed for sensitive detection of ctDNA. The novel method takes full advantages of nest HCR, which exhibited excellent analytical performance. The nest HCR products allowed a lot of AP enzymes to be captured, which led to significant enhancement of the final electrochemical signal. The biosensor exhibits high sensitivity and specificity with the low detection limit of 3 pM. More importantly, the successful implementation of this biosensor for detecting ctDNA in spiked-in serum samples, clinical pleural effusion and serum samples suggested that it is a reliable method for ctDNA detection. Furthermore, this is a convenient and cost-effective system that does not require thermal cycling procedures and complicated preparations. Above all, the developed assay may provide a useful platform for clinical detection of many kinds of meaningful ctDNA.

Declaration of competing interest

The authors declare that they have no known competing financial interests or personal relationships that could have appeared to influence the work reported in this paper.

CRediT authorship contribution statement

YiFang Huang: Conceptualization, Methodology, Writing - original draft. **MaLiang Tao:** Data curation, Visualization, Investigation. **ShiHua Luo:** Software, Validation. **Ye Zhang:** Writing - review & editing. **Bo Situ:** Writing - review & editing. **XinYi Ye:** Data curation, Software, Validation. **PeiWen Chen:** Data curation, Software, Validation. **XiuJuan Jiang:** Data curation, Software, Validation. **Qian Wang:** Supervision. **Lei Zheng:** Supervision.

Acknowledgements

This study was supported by the National Natural Science Foundation of China (81802114 and 81871735).

Appendix A. Supplementary data

Supplementary data to this article can be found online at https://doi.org/10.1016/j.aca.2020.02.006.

References

[1] H. Schwarzenbach, D.S.B. Hoon, K. Pantel, Cell-free nucleic acids as biomarkers in cancer patients, Nat. Rev. Canc. 11 (2011) 426–437, https://doi.org/

10.1038/nrc3066.
[2] C. Bettegowda, M. Sausen, R.J. Leary, I. Kinde, Y. Wang, N. Agrawal, B.R. Bartlett, H. Wang, B. Luber, R.M. Alani, E.S. Antonarakis, N.S. Azad, A. Bardelli, H. Brem, J.L. Cameron, C.C. Lee, L.A. Fecher, G.L. Gallia, P. Gibbs, D. Le, R.L. Giuntoli, M. Goggins, M.D. Hogarty, M. Holdhoff, S.-M. Hong, Y. Jiao, H.H. Juhl, J.J. Kim, G. Siravegna, D.A. Laheru, C. Lauricella, M. Lim, E.J. Lipson, S.K.N. Marie, G.J. Netto, K.S. Oliner, A. Olivi, L. Olsson, G.J. Riggins, A. Sartore-Bianchi, K. Schmidt, Ie-M. Shih, S.M. Oba-Shinjo, S. Siena, D. Theodorescu, J. Tie, T.T. Harkins, S. Veronese, T.-L. Wang, J.D. Weingart, C.L. Wolfgang, L.D. Wood, D. Xing, R.H. Hruban, J. Wu, P.J. Allen, C.M. Schmidt, M.A. Choti, V.E. Velculescu, K.W. Kinzler, B. Vogelstein, N. Papadopoulos, L.A. Diaz, Detection of circulating tumor DNA in early- and late-stage human malignancies, Sci. Transl. Med. 6 (2014) 224ra24, https://doi.org/10.1126/scitranslmed.3007094.
[3] K.C.A. Chan, P. Jiang, Y.W.L. Zheng, G.J.W. Liao, H. Sun, J. Wong, S.S.N. Siu, W.C. Chan, S.L. Chan, A.T.C. Chan, P.B.S. Lai, R.W.K. Chiu, Y.M.D. Lo, Cancer genome scanning in plasma: detection of tumor-associated copy number aberrations, single-nucleotide variants, and tumoral heterogeneity by massively parallel sequencing, Clin. Chem. 59 (2013) 211–224, https://doi.org/10.1373/clinchem.2012.196014.
[4] T. Forshew, M. Murtaza, C. Parkinson, D. Gale, D.W.Y. Tsui, F. Kaper, S.-J. Dawson, A.M. Piskorz, M. Jimenez-Linan, D. Bentley, J. Hadfield, A.P. May, C. Caldas, J.D. Brenton, N. Rosenfeld, Noninvasive identification and monitoring of cancer mutations by targeted deep sequencing of plasma DNA, Sci. Transl. Med. 4 (2012) 136ra68, https://doi.org/10.1126/scitranslmed.3003726.
[5] S.J. Dawson, D.W.Y. Tsui, M. Murtaza, H. Biggs, O.M. Rueda, S.F. Chin, M.J. Dunning, D. Gale, T. Forshew, B. Mahler-Araujo, S. Rajan, S. Humphray, J. Becq, D. Halsall, M. Wallis, D. Bentley, C. Caldas, N. Rosenfeld, Analysis of circulating tumor DNA to monitor metastatic breast cancer, N. Engl. J. Med. 368 (2013) 1199–1209, https://doi.org/10.1056/NEJMoa1213261.
[6] K.L.G. Spindler, N. Pallisgaard, R.F. Andersen, A. Jakobsen, Changes in mutational status during third-line treatment for metastatic colorectal cancer - results of consecutive measurement of cell free DNA, KRAS and BRAF in the plasma, Int. J. Canc. 135 (2014) 2215–2222, https://doi.org/10.1002/ijc.28863.
[7] S. Sumbal, A. Javed, B. Afroze, H.F. Zulfiqar, F. Javed, S. Noreen, B. Ijaz, Circulating tumor DNA in blood: future genomic biomarkers for cancer detection, Exp. Hematol. 65 (2018) 17–28, https://doi.org/10.1016/j.exphem.2018.06.003.
[8] M. Murtaza, S.J. Dawson, D.W.Y. Tsui, D. Gale, T. Forshew, A.M. Piskorz, C. Parkinson, S.F. Chin, Z. Kingsbury, A.S.C. Wong, F. Marass, S. Humphray, J. Hadfield, D. Bentley, T.M. Chin, J.D. Brenton, C. Caldas, N. Rosenfeld, Non-invasive analysis of acquired resistance to cancer therapy by sequencing of plasma DNA, Nature. 497 (2013) 108–112, https://doi.org/10.1038/nature12065.
[9] M. Sausen, J. Phallen, V. Adleff, S. Jones, R.J. Leary, M.T. Barrett, V. Anagnostou, S. Parpart-Li, D. Murphy, Q.K. Li, C.A. Hruban, R. Scharpf, J.R. White, P.J. O'Dwyer, P.J. Allen, J.R. Eshleman, C.B. Thompson, D.S. Klimstra, D.C. Linehan, A. Maitra, R.H. Hruban, L.A. Diaz, D.D. Von Hoff, J.S. Johansen, J.A. Drebin, V.E. Velculescu, Clinical implications of genomic alterations in the tumour and circulation of pancreatic cancer patients, Nat. Commun. 6 (2015) 7686, https://doi.org/10.1038/ncomms8686.
[10] C. Demuth, K.L.G. Spindler, J.S. Johansen, N. Pallisgaard, D. Nielsen, E. Hogdall, B. Vittrup, B.S. Sorensen, Measuring KRAS mutations in circulating tumor DNA by droplet digital PCR and next-generation sequencing, Transl. Oncol. 11 (2018) 1220–1224, https://doi.org/10.1016/j.tranon.2018.07.013.
[11] M. Guo, X. Li, S. Zhang, H. Song, W. Zhang, X. Shang, Y. Zheng, H. Jiang, Q. Lv, Y. Jiang, H. Hao, Real-time quantitative RT-PCR detection of circulating tumor cells from breast cancer patients, Int. J. Oncol. 46 (2015) 281–289, https://doi.org/10.3892/ijo.2014.2732.
[12] H. Chang, Y. Zhang, F. Yang, C. Wang, H. Dong, ctDNA detection based on DNA clutch probes and strand exchange mechanism, Front. Chem. 6 (2018) 530, https://doi.org/10.3389/fchem.2018.00530.
[13] X. Hu, J. Fan, B. Duan, H. Zhang, Y. He, P. Duan, X. Li, Single-molecule catalytic hairpin assembly for rapid and direct quantification of circulating miRNA biomarkers, Anal. Chim. Acta. 1042 (2018) 109–115, https://doi.org/10.1016/j.aca.2018.08.037.
[14] R. Li, L. Zou, Y. Luo, M. Zhang, L. Ling, Ultrasensitive colorimetric detection of circulating tumor DNA using hybridization chain reaction and the pivot of triplex DNA, Sci. Rep. 7 (2017) 44212, https://doi.org/10.1038/srep44212.
[15] D. Sun, J. Lu, Z. Luo, L. Zhang, P. Liu, Z. Chen, Competitive electrochemical platform for ultrasensitive cytosensing of liver cancer cells by using nanotetrahedra structure with rolling circle amplification, Biosens. Bioelectron. 120 (2018) 8–14, https://doi.org/10.1016/j.bios.2018.08.002.
[16] W. Yun, H. Wu, X. Liu, H. Zhong, M. Fu, L. Yang, Y. Huang, Ultra-sensitive fluorescent and colorimetric detection of UO 22+ based on dual enzyme-free amplification strategies, Sensor. Actuator. B Chem. 255 (2018) 1920–1926, https://doi.org/10.1016/j.snb.2017.08.205.
[17] Y. Chang, Y. Chai, S. Xie, Y. Yuan, J. Zhang, R. Yuan, Cleavage-based hybridization chain reaction for electrochemical detection of thrombin, Analyst. 139 (2014) 4264–4269, https://doi.org/10.1039/c4an00712c.
[18] J. Zhao, S. Hu, Y. Cao, B. Zhang, G. Li, Electrochemical detection of protein based on hybridization chain reaction-assisted formation of copper nanoparticles, Biosens. Bioelectron. 66 (2015) 327–331, https://doi.org/10.1016/j.bios.2014.11.039.
[19] W. Yun, H. Wu, L. Chen, L. Yang, Dual enzyme-free amplification strategy for ultra-sensitive fluorescent detection of bisphenol A in water, Anal. Chim. Acta. 1020 (2018) 104–109, https://doi.org/10.1016/j.aca.2018.02.064.
[20] C. Ma, H. Liu, T. Tian, X. Song, J. Yu, M. Yan, A simple and rapid detection assay for peptides based on the specific recognition of aptamer and signal amplification of hybridization chain reaction, Biosens. Bioelectron. 83 (2016) 15–18, https://doi.org/10.1016/j.bios.2016.04.030.
[21] X. Wang, A. Jiang, T. Hou, H. Li, F. Li, Enzyme-free and label-free fluorescence aptasensing strategy for highly sensitive detection of protein based on target-triggered hybridization chain reaction amplification, Biosens. Bioelectron. 70 (2015) 324–329, https://doi.org/10.1016/j.bios.2015.03.053.
[22] M. Xiong, Q. Rong, G. Kong, C. Yang, Y. Zhao, F.L. Qu, X.B. Zhang, W. Tan, Hybridization chain reaction-based nanoprobe for cancer cell recognition and amplified photodynamic therapy, Chem. Commun. 55 (2019) 3065–3068, https://doi.org/10.1039/c8cc10074h.
[23] J. Chen, H.H. Yang, W. Yin, Y. Zhang, Y. Ma, D. Chen, Y. Xu, S.Y. Liu, L. Zhang, Z. Dai, X. Zou, Metastable dumbbell probe-based hybridization chain reaction for sensitive and accurate imaging of intracellular-specific MicroRNAs in Situ in living cells, Anal. Chem. 91 (2019) 4625–4631, https://doi.org/10.1021/acs.analchem.8b05920.
[24] C. Feng, Z. Hou, W. Jiang, L. Sang, L. Wang, Binding induced colocalization activated hybridization chain reaction on the surface of magnetic nanobead for sensitive detection of adenosine, Biosens. Bioelectron. 86 (2016) 966–970, https://doi.org/10.1016/j.bios.2016.07.108.
[25] L. Jia, S. Shi, R. Ma, W. Jia, H. Wang, Highly sensitive electrochemical biosensor based on nonlinear hybridization chain reaction for DNA detection, Biosens. Bioelectron. 80 (2016) 392–397, https://doi.org/10.1016/j.bios.2016.02.007.
[26] F. Ma, B. Sun, H. Qi, H. Zhang, Q. Gao, C. Zhang, A signal-on electrogenerated chemiluminescent biosensor for lead ion based on DNAzyme, Anal. Chim. Acta. 683 (2011) 234–241, https://doi.org/10.1016/j.aca.2010.10.030.
[27] S. Bi, S. Yue, S. Zhang, Hybridization chain reaction: a versatile molecular tool for biosensing, bioimaging, and biomedicine, Chem. Soc. Rev. 46 (2017) 4281–4298, https://doi.org/10.1039/c7cs00055c.
[28] G. Xu, H. Zhao, J. Reboud, J.M. Cooper, Cycling of rational hybridization chain reaction to enable enzyme-free DNA-based clinical diagnosis, ACS Nano. 12 (2018) 7213–7219, https://doi.org/10.1021/acsnano.8b03183.
[29] Q. Zhou, J. Zheng, Z. Qing, M. Zheng, J. Yang, S. Yang, L. Ying, R. Yang, Detection of circulating tumor DNA in human blood via DNA-mediated surface-enhanced Raman spectroscopy of single-walled carbon nanotubes, Anal. Chem. 88 (2016) 4759–4765, https://doi.org/10.1021/acs.analchem.6b00108.
[30] Y. Zhang, S. Luo, B. Situ, Z. Chai, B. Li, J. Liu, L. Zheng, A novel electrochemical cytosensor for selective and highly sensitive detection of cancer cells using binding-induced dual catalytic hairpin assembly, Biosens. Bioelectron. 102 (2018) 568–573, https://doi.org/10.1016/j.bios.2017.12.010.
[31] X. Liu, Y. Qin, C. Deng, J. Xiang, Y. Li, A simple and sensitive impedimetric aptasensor for the detection of tumor markers based on gold nanoparticles signal amplification, Talanta. 132 (2015) 150–154, https://doi.org/10.1016/j.talanta.2014.08.072.
[32] D. Xu, D. Xu, X. Yu, Z. Liu, W. He, Z. Ma, Label-free electrochemical detection for aptamer-based array electrodes, Anal. Chem. 77 (2005) 5107–5113, https://doi.org/10.1021/ac050192m.
[33] P. Hu, S. Zhang, T. Wu, D. Ni, W. Fan, Y. Zhu, R. Qian, J. Shi, Fe–Au nanoparticle-coupling for ultrasensitive detections of circulating tumor DNA, Adv. Mater. 30 (2018), e1801690, https://doi.org/10.1002/adma.201801690.
[34] E. Gormally, E. Caboux, P. Vineis, P. Hainaut, Circulating free DNA in plasma or serum as biomarker of carcinogenesis: practical aspects and biological significance, Mutat. Res. Rev. Mutat. Res. 635 (2007) 105–117, https://doi.org/10.1016/j.mrrev.2006.11.002.